Regan, E. M., Taylor, A., May, P. W., Uney, J. B., Dick, A. D., & McGeehan, J. P. (2011). Spatially controlling neuronal adhesion and inflammatory reactions on implantable diamond. *IEEE Journal of Emerging and Selected Topics in Circuits and Systems*, *1* (4), 557 - 565. https://doi.org/10.1109/JETCAS.2011.2174469

Spatially controlling neuronal adhesion and inflammatory reactions on implantable diamond

Edward M. Regan, Alice Taylor, James Uney, Andrew D. Dick, Paul May, Joe McGeehan.
University of Bristol, UK

***Abstract*— The mechanical and chemical properties of diamond and diamond-like carbon (DLC) coatings make them very suitable materials for improving the long-term performance of invasive electrode systems used in brain-computer interfaces (BCIs). We have performed *in vitro* testing to demonstrate methods for spatially directing neural cell growth and limiting the detrimental attachment of cells involved in the foreign body response on boron-doped diamond and DLC. Inkjet-printing, laser micro-machining and stencil-assisted patterning techniques were used to control neuronal adhesion and modify inflammatory cell attachment. This work presents micro-tailored materials that could be used to improve the long-term quality of recorded signals from neural-electronic interfaces.**

***Index Terms*— Diamond, brain-computer interface, glia, neuron.**

I. Introduction

The achievements to date in brain-computer interfaces (BCI) research have generated translational promise, imagination and media attention. The attractive possibility of being able to restore function and independence to sufferers of spinal injury, degenerative disorders, *e.g.* amyotrophic lateral sclerosis, cerebrovascular disease, such as brainstem stroke, cerebral palsy and many other neuromuscular disorders drives the need for advancing neural interface technologies [1,2]. Human trials, such as the "Braingate" project (Cyberkinetics, 2004), have successfully implanted electrode arrays directly into the motor cortex of patients. These systems have produced some of the highest levels of mental control over a BCI to date, with users able to control a computer cursor, to open simulated e-mail and operate devices such as a television, even whilst conversing [2]. Despite such advances in intra-cortical implants, brain interfaces still have significant limitations restricting their functionality and longevity, including inadequate electrode resolutions and inflammatory tissue responses.

The foreign body response is an important factor in limiting the long-term functionality of multi-electrode systems implanted in to the mammalian central nervous system (CNS) [3]. Typically, around 40 - 60% reductions in the number of active electrodes have been demonstrated in multiple animal studies over a 6 month period [4,5,6,7]. Histological analyses following cortical implant insertion have shown encapsulation of the implant by activated microglia and astrocytes in a process known as glial scarring [3]. Evidence suggests that microglia mediate this response by becoming activated upon contact with many of the materials used in current implanted electrodes [8]. Improving neuron-electrode connectivity by reducing microglial activation and the subsequent scarring around neural implants has therefore become an important area of BCI research. In addition, neuronal patterning techniques provide the opportunity to control neuronal projections and direct specific neural pathways to particular electrodes.

Directed neuronal growth, by infusing neurotrophic growth factors or by placing pieces of sciatic nerve into glass microelectrodes, has been shown to promote the ingrowth of neuronal processes *in vivo* [9]. In these studies, the recorded signal:noise ratios (SNR) were often 5–10 times higher than that obtained with wire and silicon electrode arrays [3,9]. We therefore expect that an ordered system of neural cell patterning, whilst reducing glial scarring, should improve the recorded signal quality and advance BCI performance.

A variety of techniques have been developed for patterning cellular growth. The most commonly used methods include micro-contact printing, photolithography, inkjet printing and stencil-assisted patterning techniques. Generally, these techniques involve patterning proteins or factors that either attract (extra-cellular matrix proteins, polylysine) or repel (antibiofouling agents) cellular attachment, although some techniques have focused on the direct placement of cells [10,11]. Micro-contact printing (μCP) has been used to produce patterns of laminin and polylysine for spatially directing the growth of primary neurons (hippocampal and

Manuscript received June 15, 2011. This work was supported by Micron Foundation.

Edward M. Regan is with the Department of Chemistry, University of Toronto, Ontario, Canada. (E-mail: ed_regan@hotmail.com).

Alice Taylor is with the School of Chemistry, University of Bristol, UK.

Andrew Dick is with the School of Clinical Sciences, University of Bristol.

Paul May is with the School of Chemistry, University of Bristol (Tel: +44 (0)117 9289927. Fax: +44 (0)117 9251295, e-mail: Paul.May@bristol.ac.uk).

Joe McGeehan is with the Centre for Communications Research, Department of Electrical and Electronic Engineering, University of Bristol, UK. (e-mail: J.P.McGeehan@bristol.ac.uk).

cortical) on many different substrates, including glass, polystyrene and diamond [12-15]. Despite its successes, μCP has some limitations. For example, the recipient substrate has to be planar and should not be softer than the stamp material. The concentrations of transferred protein may also vary across the pattern, depending on the degree of contact between areas of the stamp and the recipient substrate (this could be affected by a non-homogenous surface roughness, topology or wettability).

Drop-on-demand inkjet printing has been widely used for depositing patterns of liquids and suspensions onto surfaces at micrometre-scale resolutions (2-50μm spot sizes [16]). Although photolithography and μCP techniques can provide better spatial resolutions, they require the construction of an unalterable master pattern and so lack the programmable versatility of inkjet printing. Additionally, the low cost and pattern reproducibility make it a very useful fabrication technique. Inkjet-printed polylysine and collagen patterns (with dot resolutions of 65 μm) have been used to direct the adhesion of primary rat hippocampal and cortical neurons, with no obvious detriment to the electrophysiology of the cells [17].

To achieve reduced levels of glial scarring and spatially controlled growth of neurons on implants, we have looked to diamond and DLC to provide the base materials for neural implant coatings. The chemical and wear resistances of diamond and DLC coatings can provide implants with protection from the harsh enzymatic and degradative environment of the body. Diamond-based coatings have also been shown to improve haemocompatability (by reducing activation of the coagulation cascade, platelets and inflammatory cells) [18-23]. Furthermore, diamond and DLC can be modified with dopant materials to alter their mechanical, chemical, electrical and biological properties [24-29]. For example, boron-doping vastly increases the electrical conductivity of diamond, making it more suitable for electrode applications [24]. Similarly, phosphorus doping of DLC has been shown to increase its conductivity by up to seven orders of magnitude [30]. Despite its obvious potential, few studies to date have explored the interaction of diamond and DLC coatings within neural systems *in vivo*. However, some non-neural *in vivo* studies have demonstrated DLC-coated implants to be well tolerated [22,23]. For example, the implantation of DLC-coated titanium into the skeletal muscle of rabbits showed no debris and no obvious acute or chronic inflammation to be present after one year [22]. I*n vitro* studies also show that diamond-based substrates can support healthy neural cell growth, providing additional evidence for the potential suitability of these materials for neural implantation [15,31]. Interestingly, diamond surfaces have been used to modulate the differentiation of neural stem cells which highlights another potential use of diamond in neural tissue engineering and implantable repair conduits [32].

We have previously demonstrated the doping of DLC with phosphorus to increase its neuronal compatibility *in vitro* [33]. In addition, we have used stencil-assisted and photochemical patterning techniques to spatially control neural cell growth on DLC [34]. Here, we extend these findings and compare the cell patterning performance of inkjet printing and the programmable and higher resolution technique of laser etching to produce neuronal networks on DLC and boron-doped diamond. Both methods are highly adaptable with regard to the patterns that can be produced and the substrates that can be modified.

We also functionalise the surface of DLC with the antifouling agents polyethylene glycol (PEG) and poly-2-hydroxyethyl methacrylate (pHEMA) to reduce inflammatory reactions in a well characterized *in vitro* glial scarring model. These materials are known for their ability to resist protein adsorption and microglial attachment, factors thought to be important in initiating the foreign body response [8,35-38]. PEGylated, micro-patterned DLC substrates are used to spatially control the adhesion of inflammatory cells (principally myeloid cells such as macrophages and CNS microglia). Our aim is to produce micro-tailored coatings that can make use of the beneficial effects of the inflammatory response, *e.g.* maintenance of the blood-brain barrier and removal (phagocytosis) of harmful cell debris from wound injury, whilst reducing glial encapsulation directly surrounding device electrodes.

As well as highlighting laser micro-machining as a novel, high resolution method for patterning neurons, this is also the first example of micropatterning antifouling coatings on diamond-based materials to spatially direct the adhesion of inflammatory cells. It is hoped that the coating strategies shown here can be used to advance future BCIs by improving neuronal connectivity to implanted intra-cortical micro-electrode arrays.

II. METHODS

A. Diamond and DLC substrates

A variety of diamond-based materials were fabricated in this study to investigate neural and inflammatory cell responses. Coatings of B-doped CVD diamond, DLC, P-doped DLC (P:DLC) and micropatterned P:DLC-DLC were deposited on to either borosilicate glass, silicon or NiCr wire substrates.

Boron-doped diamond films were grown in a standard hot filament chemical vapour deposition (CVD) reactor using CH_4/H_2 process gases at a pressure of 20 Torr. The substrate was undoped single-crystal (100) Si, abraded ultrasonically before deposition using a slurry of 100 nm diamond grit in water. Rhenium was used for the filament material with the filament temperature kept constant at 2400 °C and monitored using a 2-colour optical pyrometer. The substrate temperature was maintained at ~ 900 °C. Diborane (B_2H_6) gas diluted in H_2 was used as the source of B at concentrations of 0~1000 ppm with respect to CH_4. All three gases were metered into the chamber using mass flow controllers. The resulting diamond films were around 3-4 μm thick over an area ~ 1 cm^2.

The films were polycrystalline, with a facetted morphology having crystal sizes on the surface of ~ 1 μm. Varying the B content in the gas mixture, and hence in the films, allowed the conductivity of the films to be controllably altered between extremely insulating (resistivity of MΩ.cm) to near metallic (resistivity of a few Ω.cm). After deposition, the films were oxidised by exposure to UV-irradiation/ozone for 20 minutes using a UV-O cleaner (Jetlight Company, 42A-220).

For preparation of the DLC and P:DLC samples a pulsed laser deposition (PLD) set-up was used, as previously described in [24]. The targets were comprised of either a graphite disk (Poco Graphite Inc., DFP-3-2 grade), or compressed disks of graphite and red phosphorus (20 at. %) powder mixtures.

Micropatterned P:DLC-DLC substrates were prepared by initially coating glass coverslips (13 mm diameter) with P:DLC for 600 laser shots. Copper transmission electron microscope (TEM) grids (PL200 parallel lines, 50 μm spacing, Agar Scientific) were then used as shadow masks and the substrates were coated with DLC for a further 600 laser shots. Coverslips were subjected to 20 minutes of sonication in acetone and methanol, before being washed in deionised water overnight. Samples were then air-dried and stored in an airtight container until use.

B. PEGylated DLC substrates

Spatially directed PEGylation was produced using micropatterned P:DLC-DLC films to determine if these substrates could be used to pattern the adhesion of cells involved in inflammatory responses.

Micropatterned P:DLC-DLC substrates were incubated with poly-D-lysine (1 mg.mL^{-1}, Sigma) for 1 hour, washed three times in distilled water and air dried. Substrates were then immersed in 10 μL of a 250 mM TMS–PEG12–NHS ester (Pierce Biotechnology) solution diluted in 50:50 DMSO (Sigma):borate buffer (pH 8.5, 50 mM, Thermo Scientific). The substrates were washed copiously with PBS (10 minute washes, × 6) and stored in PBS before use.

C. Inkjet printing

Inkjet printing was used to fabricate micropatterned polylysine onto P:DLC surfaces to investigate whether these substrates could support patterned neuronal growth.

P:DLC coated coverslips (13 mm) and micro-electrode arrays (MEA, Multichannel Systems, 6 × 10 configuration) were printed on using a Dimatix DMP-2800 printer (Fuji, Japan). The inkjet print solution consisted of FITC-labeled poly-L-lysine (MW 15000-30000, Sigma, UK) dissolved in 50:50 ethanol:water to produce a final concentration of 2.5 mg.mL^{-1}. After printing, a culture well was glued on to the MEA using silicone adhesive (3145 RTV MIL-A-46146 CLEAR, Dow Corning). Printed glass coverslips (n = 6) and the MEA substrates (n = 3) were then taken to a sterile culture hood and sterilised in ethanol. Substrates were dried in air and placed into culture dishes (24-well plates/100mm × 25mm Petri dish, Thermo-Fisher).

D. pHEMA-coated substrates

The antibiofouling agent, pHEMA, was coated onto P:DLC coated coverslips and NiCr wires to investigate the ability of these substrates to reduce macrophage adhesion and inflammatory responses in an *in vitro* model of glial scarring.

P:DLC coverslips were placed into 24-well culture plates (Nunc) and 300 μL of pHEMA solution (120 mg.mL^{-1} in 95% ethanol) was pipetted on. The solution was immediately pipetted off and left to dry in an oven at 60º C.

P:DLC-coated NiCr microwires (50 μm thickness, A-M Systems) were cut into 3–5 mm pieces and soaked in 70% ethanol for at least 30 min and dried in a laminar hood. The pHEMA-coated P:DLC wires were prepared by dipping them into a solution of pHEMA (10g.mL^{-1}, Sigma, UK) for 10 seconds and were then left to dry at 60º C.

E. Laser etching

The laser etching of polylysine-coated, B-doped diamond surfaces was used to fabricate a micro-patterned polylysine surface. These substrates allowed us to investigate whether laser-etched diamond could mediate spatially controlled neuronal growth.

An Nd:YAG laser (532 nm) micro-machining system (Alpha, Oxford Lasers, UK) was used to etch patterns into the surface of the boron-doped CVD diamond substrates. Samples were initially coated with poly-D-lysine (0.1 mg.mL^{-1}, Sigma, UK) for 1 hour, washed three times in deionised water and dried in air. A sequence of 10 connecting rectangles (100 μm height, 1000 μm length) was etched using a laser power of 30% (0.8 W over an area ~ 80 μm). Samples were sterilised by immersing the substrates in a 10% (v/v) penicillin-streptomycin-amphotericin B (PSA) solution (in PBS, Sigma), washed in deionised water three times and air-dried.

F. Cortical neurons

Cortical neurons were cultured on substrates using standard tissue culture protocols, as described in [39]. Briefly, substrates were sterilised in ethanol and coated with poly-D-lysine (70,000–150,000 MW, Sigma) for 1 hour (0.1 mg.mL^{-1}) and washed three times in sterilised, deionised water (20 minutes for each wash). Neuron-rich cultures were produced by isolating the cerebral cortices from the pups of embryonic day 18 (E18) Wistar rats. The meninges were carefully removed and the cortical tissue dissociated by protease digestion using 10% (v/v) trypsin for 20 min. The tissue was triturated using a fire-polished Pasteur pipette to produce a homogeneous single-cell suspension. Cells were diluted in Neurobasal medium™ containing 2% B-27, L-glutamine (0.5 mmol.L^{-1}, Sigma, UK) glutamic acid (25 μmol.L^{-1}, Sigma, UK) , penicillin (100 U.mL^{-1}, Sigma, UK), streptomycin (100 μg.ml^{-1}) and seeded at a concentration of 1×10^5 cells per well on P:DLC and boron-doped diamond substrates. A lower cell density of 2.5×10^4 cells per well was used for the MEAs. The cell cultures were placed in an incubator at 37 °C/5% CO_2 and fed at 3 day intervals by replacement of half of the medium

(minus glutamic acid). Cells were then fixed at 5-7 days *in vitro* with 4% paraformaldehyde (PFA, in PBS) for 20 min, washed with PBS and photographed using an imaging system (Leica, Swizerland).

G. Bone-marrow derived macrophages

Bone marrow-derived macrophages were generated from C57BL/6 mice as described in [40]. In brief, bone marrow cells were washed in DMEM media and resuspended at 1×10^5 cells mL^{-1} in complete medium supplemented with 5% horse serum (PAA, UK) and 50 $pg.mL^{-1}$ macrophage-colony stimulating factor (produced by Mr D. Copland, University of Bristol). The cell suspension (50 mL) was transferred to Teflon-coated tissue culture bags (supplied by Dr. M. Munder, University of Heidelberg, Germany) and incubated for 8 days at 37ºC in 5% CO_2. Cells were removed from the Teflon bags and centrifuged and the cell pellet resuspended in culture media consisting of DMEM without phenol red (PAA, UK) supplemented with 10% heat-inactivated fetal calf serum (FCS, TCS Cellworks, UK), 100U mL^{-1} penicillin-streptomycin (Invitrogen, UK), L-glutamine (2 $mmol.L^{-1}$, Invitrogen, UK), sodium pyruvate (1 $mmol.L^{-1}$, Invitrogen, UK), and 2-mercaptoethanol (5×10^{-5} $mol.L^{-1}$, (Invitrogen, UK).

This cell suspension was plated onto (i) PEGylated, micropatterned DLC substrates, (ii) P:DLC-coated glass coverslips and (iii) pHEMA-coated P:DLC substrates. The coverslips were placed inside 24-well, flat-bottomed plates (polystyrene multidish, Nunc) and cells seeded at a density of 2.5×10^5 cells per well (n = 9, using 3 separate cultures). Cells were fixed at 3 days *in vitro* for PEGylated micropatterned DLC substrates and at 1 day *in vitro* for the P:DLC/pHEMA substrates using 4% PFA (in PBS, pH 7.2) for 20 min. Cells were washed with PBS and photographed using an imaging system (Leica, Switzerland). For cell counting, the cells were stained with 4',6-diamidino-2-phenylindole (DAPI, Thermo-Fisher) and three images per sample (n = 9 samples) were taken. Each image covered an area of 700 µm × 550 µm. Cell count data were averaged and normalized to cells per mm^2.

H. In vitro glial scarring model

A mixed culture containing neurons, astrocytes and microglia was used to a produce an *in vitro* model of glial scarring, as previously described by Polikov [41]. This model allowed us to test the effects of pHEMA-P:DLC coatings on glial and neuronal responses and to simulate the effects of these coatings *in vivo*.

Neuron–glia cultures were prepared from the ventral mesencephalic tissues of embryonic day 15 Sprague Dawley rats, as described in [41] with some modifications. Briefly, dissociated cells were seeded at 5×10^5 cells per well into poly-D-lysine-coated 24-well plates (Nunc), using the same coating procedure as described for cortical neurons. Cells were grown in Neurobasal (NB) medium supplemented with 2% B-27, 2 mM L-glutamine, 50 $U.mL^{-1}$ penicillin, 50µg.mL^{-1} streptomycin and 10 $ng.mL^{-1}$ of bFGF. At 10 days, the media was changed to NB with B-27, 10% FBS, 2mM L-glutamine, 50 $U.mL^{-1}$ penicillin, and 50µg.mL^{-1} streptomycin. P:DLC-coated and P:DLC:pHEMA-coated wires were placed into each well at random locations using sterile forceps, so that the pieces would sink and rest atop the cultured cell layer. Media changes were performed every 3 days by replacement of half the media. Cultures were fixed with 4% PFA 7 days after the wires were added (17 days *in vitro*, n = 9 using 3 separate cultures).

I. Immunocytochemistry

Fluorescence labeling of rat cortical neurons was performed using a monoclonal mouse antibody to beta-III-tubulin (ABCAM, UK). Cultures fixed with 4% PFA were aspirated and washed for 5 minutes (× 3) in PBS. Cell membranes were permeabilised with 5 minute washes (× 3) using 0.5% (v/v) Triton X100 (Sigma). A blocking solution of 10% normal donkey serum (NDS, v/v) in PBS was added for 30 minutes. Cells were incubated with the beta-III-tubulin antibody (1:400 in PBS) for 1 hour at room temperature and for a further 12 hours at 4 ºC. Cells were washed for 5 minutes (× 3) in PBS with 0.5% Triton-X100, followed by incubation with the secondary anti-mouse conjugated with Cy2 (1:250; Jackson Laboratories, USA) in PBS with 0.5% NDS (v/v) and 0.1% Triton X-100 (v/v) for 2 hours at room temperature. Cells were washed for 5 minutes (× 3) in PBS before being counterstained with 0.5 $mg.mL^{-1}$ DAPI (Thermo-Fisher). Coverslips were finally washed in PBS for 5 minutes (× 3) and mounted face-down onto 76 mm × 26 mm microscope slides using a droplet (20 µm) of Vectashield™ non-quenching mounting medium. Staining was visualised using an inverted imaging system (Leica, Switzerland, λ_{ex} = 492nm, λ_{em} = 510 nm).

For immunocytochemistry of the glial scarring model samples, dual staining of neurons and glia was performed. This was achieved using the same protocol as above but with the addition of a polyclonal anti-rabbit antibody reactive to the glial marker, GFAP (ABCAM, UK). For the secondary antibody step, an additional anti-rabbit conjugated with Cy3 (1:200; Jackson Laboratories, USA) was also added to the PBS with 0.5% NDS (v/v) and 0.1% Triton X-100 (v/v) solution.

III. RESULTS

A. Neuronal patterning

Inkjet printing and laser micro-machining were used to control the spatial distribution of neurons on P-doped DLC (P:DLC) and B-doped diamond. Both techniques require control of the spatial distribution of polylysine (PL), a cationic polymer used to promote neuronal adhesion. Our previous work had already demonstrated that PL-coated P:DLC substrates allow very good adhesion and growth of neurons *in vitro* [17]. We therefore wanted to test if printed PL produced good levels of neuronal adherence on P:DLC and if neurons adhered similarly to PL-coated boron-doped diamond.

For inkjet printing, FITC-tagged PL was deposited within a solution of ethanol and water (50:50, v/v) on to P:DLC substrates. The ethanol facilitated the ejection of droplets from the inkjet print heads, probably by reducing the surface tension of the solution. Dot arrays of PL (100 × 100) were deposited on to P:DLC with single spot sizes of ~ 50μm and pitch spacings of 200 μm. Rat cortical neurons plated on to these substrates adhered mostly to PL-printed areas, sometimes extending neuritic processes out to adjacent 'islands' of cells (Fig. 1, A). Neurons grew firmly as a monolayer on the surface (Fig. 1, B) with the position of cells, in general, following the location of the printed PL dots, as visualized by fluorescence microscopy (Fig. 1, C).

This method was also applied to pattern neurons on to a planar electrode array. Previous studies have patterned neurons on to planar electrode arrays to simplify neuronal growth and thereby aid the investigation of neural networks [42]. Developments in neuronal network growth on MEAs are likely to provide an increasingly important tool for understanding how computational processes like memory and data processing occur within neural systems. We used our inkjet printer to deposit parallel lines of PL across the electrode line of a commercially available MEA. Fig. 1D shows an image of neurons adhering to and forming a dense neuritic mass across the PL-printed line. The lines were approximately 50 μm thick and 400 μm long. Small levels of non-compliant growth were observed in non-printed areas, likely due to some 'splashing' of the PL solution during printing. However, the majority of neuronal processes occurred within the printed area, highlighting the potential use of this method for *in vitro* neural network studies.

Our laser micro-machining method offers spatial resolutions of ~ 10 μm and, like inkjet printing, patterns can be easily programmed and fabricated. B-doped diamond was initially coated with PL and areas were then laser etched away. Firstly, it was important to assess whether B-doped diamond substrates would allow neuronal adhesion when coated with PL. Neuronal growth was compared on PL-coated, B-doped diamond and the control substrate, tissue culture polystyrene (TCPS), with representative sample images shown in Fig. 2 (A and B). Immunostaining was required to adequately visualise the neurons on the opaque diamond samples. Neurons expressed the neuronal marker, beta-III-tubulin, and adhered well on the B-doped diamond. Large numbers of neuritic processes were extended up to at least 7 days *in vitro* (Fig. 2A). The cell growth on B-doped diamond appeared very similar to that observed on the control TCPS substrates, indicating that both substrates could support healthy neuronal growth (Fig. 2B). This result is in line with our previous studies where cell counts on B-doped diamond do not statistically differ to that observed on undoped diamond or TCPS [43].

Laser micro-machining was used to etch arrays of 10 connected rectangles (each 100 μm × 1000 μm) into the PL-coated, B-doped diamond. Light microscopy measurements determined that the thickness of each etched line was ~ 10 μm. The patterns produced were visible under the optical microscope, probably due to some graphitisation of the diamond surface. Rat cortical neurons grew well across the unetched, PL-coated areas and neuritic outgrowth largely avoided crossing over the etched areas. This avoidance made the etched pattern visible upon staining of the cells and their processes (Fig. 2 C and D). It is probable that the destruction of the PL in the etched areas was responsible for mediating the patterned neuronal growth. However, potential effects on cell adhesion from an alteration in the diamond structure, *e.g.* graphitisation, at the etched areas cannot be excluded.

B. pHEMA coatings on P:DLC

The pHEMA solution was coated on to P:DLC-coated glass coverslips to form a semi-transparent layer (~ 100 μm thick). Bone marrow derived macrophage (BMDM) cultures were used to model the adhesion and growth responses of CNS microglia (and infiltrating macrophages during a foreign body inflammatory response) on these substrates. Unlike neurons, BMDMs adhere to nearly all surfaces without the need for additional coating polymers such as PL. It was therefore hoped that we could reduce their adhesion using pHEMA, a known antifouling agent. Coating the P:DLC substrates with pHEMA produced a significant effect on reducing their adhesion, with 98-99% fewer adhered cells compared with uncoated P:DLC (Fig. 3). The number of adhered cells on glass and P:DLC were similar with no statistically significant differences (analyses were determined by one-way ANOVA with Bonferroni's multiple comparison test).

A well characterised *in vitro* glial scarring model [41] was used to simulate the foreign body response to implanted electrodes. This model involved growing a mixed culture of neurons, astrocytes and microglia isolated from embryonic (day 15) rat brain. Earlier studies using this model have demonstrated that both microglia and astrocytes migrate to and form a glial barrier around stainless steel wires, placed directly onto the cell layer. This reaction bears great similarity to *in vivo* glial scar responses to implanted electrodes. In our study, placing P:DLC-NiCr microwires (50 μm thickness) on to the culture resulted in gradual increases over time in the number of cells surrounding their edges. NiCr wires were selected as an alternative to stainless steel wires since both materials are typically used for *in vivo* electrode applications [44]. After 10 days, the areas adjacent to the wire were observed to have an obvious accumulation of cells along the length of the microwire (Fig. 4A). Previous studies suggest that these cells consist mainly of microglia and astrocytes [41] and our immunocytochemistry results confirm the build-up of astrocytes surrounding the P:DLC-coated NiCr wires and neurons around the 'scar' (Fig. 4C). Staining for neurons and glia on culture wells without a wire was also performed to show the typical presence of both astrocytes and neurons throughout the well area (Figure 4D). Similar observations were noted with non-coated NiCr wires (data not shown). The accumulation of cells was, however, not observed around any

pHEMA-coated P:DLC-NiCr microwires (Fig. 4B), showing that pHEMA coatings could markedly reduce the glial scarring responses in this model.

C. TMS-PEG coatings on micropatterned DLC

As an alternative approach to controlling macrophage adhesion, we tested a PEGylation method that uses the TMS-PEG-NHS ester reagent to add PEG groups to the surface of PL-coated P:DLC. Our previous work has shown that PL adsorbs well on to P:DLC, but poorly on to DLC [24]. We therefore used this property to spatially control areas of PEGylation by micropatterning the P:DLC and DLC. The structure of the functionalised layers on P:DLC is shown in Fig. 5. Parallel-line masks were used to define areas of DLC and P:DLC on glass coverslips. Light microscopy images of the micropatterned P:DLC-DLC substrates are shown in Fig. 6. BMDMs were plated onto these substrates and were photographed at 3 days *in vitro*. The cells displayed a regular morphology with only very few cells adhering to the PEGylated P:DLC areas. In contrast, many cells adhered to the non-PEGylated DLC surface (Fig. 6), showing that this method is effective at spatially controlling the adhesion of macrophages.

IV. Conclusion

This study has assessed various strategies for patterning neural and inflammatory cells on diamond-based coatings. We have reported and compared inkjet printing and laser micromachining as programmable, automated and high-throughput methods for spatially controlling neuronal growth *in vitro*. Our findings show that both techniques can be used to successfully pattern neurons and cell-adhesion molecules on to diamond surfaces. Our inkjet-printed polylysine patterns produced dot resolutions of ~ 50 μm, which is an improvement on previous studies that have reported dot resolutions of 65-300 μm [45,46]. Laser micro-machining has the advantage of further improved dot resolutions of ~ 10 μm. We hope to apply and develop these findings to guide neuronal growth *in vivo* and to use these methods to facilitate *in vitro* neural network studies.

We have also demonstrated two antibiofouling coating strategies for controlling macrophage adhesion and inflammatory responses within a well characterised *in vitro* model of glial scarring. Our findings provide evidence that reducing inflammatory cell adherence using antifouling coatings, like pHEMA, can reduce the accumulation of glia surrounding devices implanted into the CNS. Whilst, other studies have reported similar low levels of inflammatory cell adherence (monocytes and macrophages) using antifouling agents [8,25,36], we have presented the additional possibility of spatially controlling this effect using our micropatterned PEG surfaces. We believe that by doing so, we can tailor implants that make use of the beneficial effects of the foreign body response (*e.g.* reduced susceptibility to infection and removal of harmful debris [45]), whilst reducing the negative effects on neuron-electrode connectivity demonstrated in many chronically implanted electrode studies [4,5,6,7] (see Fig. 8 for a schematic diagram and explanation of this concept).

In future studies, we intend to micropattern pHEMA, which other studies have already shown to be amenable to surface patterning [46], and test inflammatory cell responses and neuronal growth on patterned pHEMA coatings. We believe that both PEG and pHEMA each have unique properties that provide advantages for different implant applications. For example, the PEG coatings are thin and so would provide low electrical resistance to adjacent neurons whilst potentially reducing microglial adhesion and activation. However, pHEMA is a hydrogel that can be applied as a thicker coating that could provide a soft, mechanical buffer between hard electrode devices and soft brain tissue. This buffer could reduce neural cell damage surrounding an implant whilst also providing a non-inflammatory surface.

Further applications for this work include the possibility of controlling the spatial distribution of macrophages to influence macrophage activation on implanted surfaces. Indeed, topological and chemical patterning of substrates have been well documented to influence macrophage activation, morphology and phenotype [47,48]. For example, the diameter of single dots of titanium within an array pattern were shown to influence the level of reactive oxygen species (ROS) produced by macrophages and neutrophils [48]. Interestingly, smaller diameter dot patterns (5 μm) produced a significant decrease in ROS, compared with larger dot sizes (10, 30, 100 μm). Patterned surfaces also provide an excellent platform for mimicking the complexity of the glycocalyx and investigating cell-cell interactions and the cell-surface interface.

We have focused on using these deposition techniques on modified diamond and DLC, materials well known for their exceptional resistance to physical wear and chemical corrosion [49,50]. Our study has demonstrated significant neuronal adhesion with cells that maintain their characteristic morphology on both boron-doped diamond and P:DLC. Given the data we present here, further study is warranted to determine the effects of laser etching on substrate properties, such as surface roughness and structural alteration. To date, our observations strongly suggest that patterns of polymers like PL can be etched away to form a spatially defined substrate for organising neural cell growth. We believe that any degree of spatial organisation of neuronal growth processes would benefit neuro-interface technologies. Since laser ablation techniques have been reported to achieve sub-micron resolutions [51], we would predict that our technique could be used to pattern individual neuritic processes and single cell somata in the near future.

We intend to extend this work to assess the performance and longevity of our microtailored substrates *in vivo*. Both PEG and pHEMA have been used in FDA-approved medical devices in the CNS [52] and thus rapid clinical translation remains highly plausible as they are unlikely to produce detrimental effects upon implantation. We believe that these microtailored substrates can benefit the long-term performance of BCI interfaces by providing (i) improved levels of neuronal connectivity (ii) better organisation of the neuron-electrode interface and (iii) higher resistance to degradation. Moreover,

this work will inform and have further applications in neural network research, investigating inflammatory cell responses and in the development of nerve and brain repair scaffolds.

ACKNOWLEDGMENT

The authors would like to thank Micron Foundation for their financial support for this work programme and Dr Maeve Caldwell, Dr James Smith and Mr Tim Heal at the University of Bristol for their practical assistance and contributions.

REFERENCES

[1] Wolpaw JR, Birbaumer N, McFarland DJ, Pfurtscheller G, Vaughan TM. Brain-computer interfaces for communication and control. Clin Neurophysiol. 2002 Jun;113(6):767-91.

[2] Hochberg LR, Serruya MD, Friehs GM, Mukand JA, Saleh M, Caplan AH, Branner A, Chen D, Penn RD, Donoghue JP. Neuronal ensemble control of prosthetic devices by a human with tetraplegia.

[3] Polikov VS, Tresco PA, Reichert WM. Response of brain tissue to chronically implanted neural electrodes. J Neurosci Methods. 2005 Oct 15;148(1):1-18.

[4] Nicolelis MA, Dimitrov D, Carmena JM, Crist R, Lehew G, Kralik JD, Wise SP. Chronic, multisite, multielectrode recordings in macaque monkeys. Proc Natl Acad Sci U S A. 2003 Sep 16;100(19):11041-6.

[5] Rousche PJ, Normann RA. Chronic recording capability of the Utah Intracortical Electrode Array in cat sensory cortex. J Neurosci Methods. 1998 Jul 1;82(1):1-15.

[6] Williams JC, Rennaker RL, Kipke DR. Long-term neural recording characteristics of wire microelectrode arrays implanted in cerebral cortex. Brain Res Brain Res Protoc. 1999 Dec;4(3):303-13.

[7] Liu X, McCreery DB, Carter RR, Bullara LA, Yuen TG, Agnew WF. Stability of the interface between neural tissue and chronically implanted intracortical microelectrodes. IEEE Trans Rehabil Eng. 1999 Sep;7(3):315-26.

[8] Leung BK, Biran R, Underwood CJ, Tresco PA. Characterization of microglial attachment and cytokine release on biomaterials of differing surface chemistry. Biomaterials. 2008 Aug;29(23):3289-97.

[9] Kennedy PR, Mirra SS, Bakay RA. The cone electrode: ultrastructural studies following long-term recording in rat and monkey cortex. Neurosci Lett. 1992 Aug 3;142(1):89-94.

[10] Falconnet D, Csucs G, Grandin HM, Textor M. Surface engineering approaches to micropattern surfaces for cell-based assays. Biomaterials. 2006 Jun;27(16):3044-63.

[11] Xu T, Jin J, Gregory C, Hickman JJ, Boland T. Inkjet printing of viable mammalian cells. Biomaterials. 2005 Jan;26(1):93-9.

[12] Corey JM, Feldman EL. Substrate patterning: an emerging technology for the study of neuronal behavior. Exp Neurol. 2003 Nov;184 Suppl 1:S89-96.

[13] James CD, Spence AJ, Dowell-Mesfin NM, Hussain RJ, Smith KL, Craighead HG, Isaacson MS, Shain W, Turner JN. Extracellular recordings from patterned neuronal networks using planar microelectrode arrays. IEEE Trans Biomed Eng. 2004 Sep;51(9):1640-8.

[14] Chang JC, Brewer GJ, Wheeler BC. A modified microstamping technique enhances polylysine transfer and neuronal cell patterning. Biomaterials. 2003 Aug;24(17):2863-70.

[15] Specht CG, Williams OA, Jackman RB, Schoepfer R. Ordered growth of neurons on diamond. Biomaterials. 2004 Aug;25(18):4073-8.

[16] Sekitani T, Noguchi Y, Zschieschang U, Klauk H, Someya T. Organic transistors manufactured using inkjet technology with subfemtoliter accuracy. Proc Natl Acad Sci U S A. 2008 Apr 1;105(13):4976-80.

[17] Sanjana NE, Fuller SB. A fast flexible ink-jet printing method for patterning dissociated neurons in culture. J Neurosci Methods. 2004 Jul 30;136(2):151-63.

[18] Ma WJ, Ruys AJ, Mason RS, Martin PJ, Bendavid A, Liu ZW, et al. DLC coatings: effects of physical and chemical properties on biological response. Biomaterials 2007;28(9):1620–8.

[19] Nurdin N, Francois P, Mugnier Y, Krumeich J, Moret M, Aronsson BO, et al. Haemocompatibility evaluation of DLC- and SiC-coated surfaces. European Cells and Materials 2003;5:17–26. discussion 26–28.

[20] Jones MI, McColl IR, Grant DM, Parker KG, Parker TL. Haemocompatibility of DLC and TiC–TiN interlayers on titanium. Diamond and Related Materials 1999;8(2–5):457–62.

[21] Jones MI, McColl IR, Grant DM, Parker KG, Parker TL. Protein adsorption and platelet attachment and activation, on TiN, TiC, and DLC coatings on titanium for cardiovascular applications. Journal of Biomedical Materials Research 2000;52(2):413–21.

[22] Mohanty M, Anilkumar TV, Mohanan PV, Murakeedharan CV, Bhuvaneshwar GS, Dereangere F, Sampeur Y, Surynarayanan R. Long term tissue response to titanium coated with diamond-like carbon. Biomolecular Engineering 2002 (19), 125-128.

[23] Allen M, Myer B, Rushton N. In vitro and in vivo investigations into the biocompatibility of diamond-like carbon (DLC) coatings for orthopedic applications. Journal of Biomedical Materials Research 2001;58(3):319–28.

[24] Luong JH, Male KB, Glennon JD. Boron-doped diamond electrode: synthesis, characterization, functionalization and analytical applications. Analyst. 2009 Oct;134(10):1965-79. Review. Erratum in: Analyst. 2010 Nov;135(11):3008.

[25] Sen A, Barizuddin S, Hossain M, Polo-Parada L, Gillis KD, Gangopadhyay S. Preferential cell attachment to nitrogen-doped diamond-like carbon (DLC:N) for the measurement of quantal exocytosis. Biomaterials. 2009 Mar;30(8):1604-12.

[26] Kwok SCH, Jin W, Chu PK. Surface energy, wettability, and blood compatibility phosphorus doped diamond-like carbon films. Diamond and Related Materials 2005;14(1):78–85.

[27] Sikora A, Berkesse A, Bourgeois O, Garden J-L, Guerret-Piécourt C, Loir A-S, Garrelie F, Donnet C. Electrical properties of boron-doped diamond-like carbon thin films deposited by femtosecond pulsed laser ablation. Applied Physics A: Mat. Sci. & Processing. 2009 Jan; Vol. 94 (1): 105-109.

[28] Hasebe T, Shimada A, Suzuki T, Matsuoka Y, Saito T, Yohena S, Kamijo A, Shiraga N, Higuchi M, Kimura K, Yoshimura H, Kuribayashi S. Fluorinated diamond-like carbon as antithrombogenic coating for blood-contacting devices. J Biomed Mater Res A. 2006 Jan;76(1):86-94.

[29] Chekana NM, Beliauskia NM, Akulicha VV, Pozdniakb LV, Sergeevaa EK, Chernovb AN, Kazbanovb VV, Kulchitskyb VA. Biological activity of silver-doped DLC films. Diamond and Related Materials 2009; 18, (5-8): 1006-1009.

[30] Fuge GM, May PW, Rosser KN, Pearce SRJ, Ashfold MNR. Laser Raman and X-ray photoelectron spectroscopy of phosphorus containing diamond-like carbon films grown by pulsed laser ablation methods. Diamond and Related Materials 13 (2004) 1442–1448.

[33] Kelly S, Regan EM, Uney JB, Dick AD, McGeehan JP; Bristol Biochip Group, Mayer EJ, Claeyssens F. Patterned growth of neuronal cells on modified diamond-like carbon substrates. Biomaterials. 2008 Jun;29(17):2573-80. Epub 2008 Mar 21.

[34] Regan EM, Uney JB, Dick AD, Zhang Y, Nunez-Yanez J, McGeehan JP, Claeyssens F, Kelly S. Differential patterning of neuronal, glial and neural progenitor cells on phosphorus-doped and UV irradiated diamond-like carbon. Biomaterials. 2010 Jan;31(2):207-15. Epub 2009 Oct 14.

[35] Jenney CR, Anderson JM. Effects of surface-coupled polyethylene oxide on human macrophage adhesion and foreign body giant cell formation in vitro. J Biomed Mater Res. 1999 Feb;44(2):206-16.

[36] DeFife KM, Shive MS, Hagen KM, Clapper DL, Anderson JM. Effects of photochemically immobilized polymer coatings on protein adsorption, cell adhesion, and the foreign body reaction to silicone rubber. J Biomed Mater Res. 1999 Mar 5;44(3):298-307.

[37] Jenney CR, Anderson JM. Adsorbed serum proteins responsible for surface dependent human macrophage behavior. J Biomed Mater Res. 2000 Mar 15;49(4):435-47.

[38] Ito Y, Hasuda H, Sakuragi M, Tsuzuki S. Surface modification of plastic, glass and titanium by photoimmobilization of polyethylene glycol for antibiofouling. Acta Biomater. 2007 Nov;3(6):1024-32.

[39] Howarth JL, Kelly S, Keasey MP, Glover CP, Lee YB, Mitrophanous K, Chapple JP, Gallo JM, Cheetham ME, Uney JB. Hsp40 molecules that target to the ubiquitin-proteasome system decrease inclusion formation in models of polyglutamine disease. Mol Ther. 2007 Jun;15(6):1100-5.

[40] Munder M, Eichmann K, Moran JM, Centeno F, Soler G, Modolell M. Th1/Th2-regulated expression of arginase isoforms in murine macrophages and dendritic cells. J Immunol. 1999; 163: 3771-7.
[41] Polikov VS, Su EC, Ball MA, Hong JS, Reichert WM. Control protocol for robust in vitro glial scar formation around microwires: essential roles of bFGF and serum in gliosis. J Neurosci Methods. 2009 Jul 30;181(2):170-7. Epub 2009 May 15.
[42] Jun SB, Hynd MR, Dowell-Mesfin N, Smith KL, Turner JN, Shain W, Kim SJ. Low-density neuronal networks cultured using patterned poly-l-lysine on microelectrode arrays. J Neurosci Methods. 2007 Mar 15;160(2):317-26.
[43] A. Taylor, E. Regan, P.W. May. Mater. Res. Soc. Symp. Proc. (Fall 2011), in press.
[44] Zhang J, Wilson CL, Levesque MF, Behnke EJ, Lufkin RB. Temperature changes in nickel-chromium intracranial depth electrodes during MR scanning. AJNR Am J Neuroradiol. 1993 Mar-Apr;14(2):497-500.
[45] He W, McConnell GC, Bellamkonda RV. Nanoscale laminin coating modulates cortical scarring response around implanted silicon microelectrode arrays. J Neural Eng. 2006 Dec;3(4):316-26.
[46] Bryant SJ, Hauch KD, Ratner BD. Spatial patterning of thick poly(2-hydroxyethyl methacrylate) hydrogels. Macromolecules 2006 39 (13), 4395-4399.
[47] Bartneck M, Schulte VA, Paul NE, Diez M, Lensen MC, Zwadlo-Klarwasser G. Induction of specific macrophage subtypes by defined micro-patterned structures. Acta Biomater. 2010 Oct;6(10):3864-72.
[48] Sahlin H, Contreras R, Gaskill DF, Bjursten LM, Frangos JA. Anti-inflammatory properties of micropatterned titanium coatings. J Biomed Mater Res A. 2006 Apr;77(1):43-9.
[49] Dearnaley G. Diamond-like carbon: a potential means of reducing wear in total joint replacements. Clin Mater. 1993;12(4):237-44. Review.
[50] Booth L, Catledge SA, Nolen D, Thompson RG, Vohra YK. Synthesis and Characterization of Multilayered Diamond Coatings for Biomedical Implants. Materials (Basel). 2011 May;4(5):857-867.
[51] Ali M, Wagner T, Shakoor M, Molian PA. Review of laser nanomachining. J. Laser Appl. 20, 169 (2008).
[52] http://www.alphacor-ati.com/AlphaCor/AlphaSphere.html

Edward M. Regan received his Ph.D at the University of Bristol in 2010. The author has been a member of the "Bristol Biochip group" since 2007, who along with their industrial partner, Aptina Ltd, have been developing CMOS-based neurosensor platforms. The author's primary research has focus has been on designing biomaterial coatings for neurosensory devices. The author is now at the Department of Chemistry, University of Toronto, continuing his work with biosensor platforms and digital microfluidics. The author became a member of the Tissue and Cell Engineering Society in 2009 and the IEEE Robotics and Automation Society (RAS) Technical Committee (TC) on Bio-robotics in 2011.

Alice Taylor – Biography unavailable at time of submission.

James Uney – Biography unavailable at time of submission.

Andrew D. Dick – Biography unavailable at time of submission.

Paul May – Biography unavailable at time of submission.

Joe McGeehan. – Biography unavailable at time of submission.

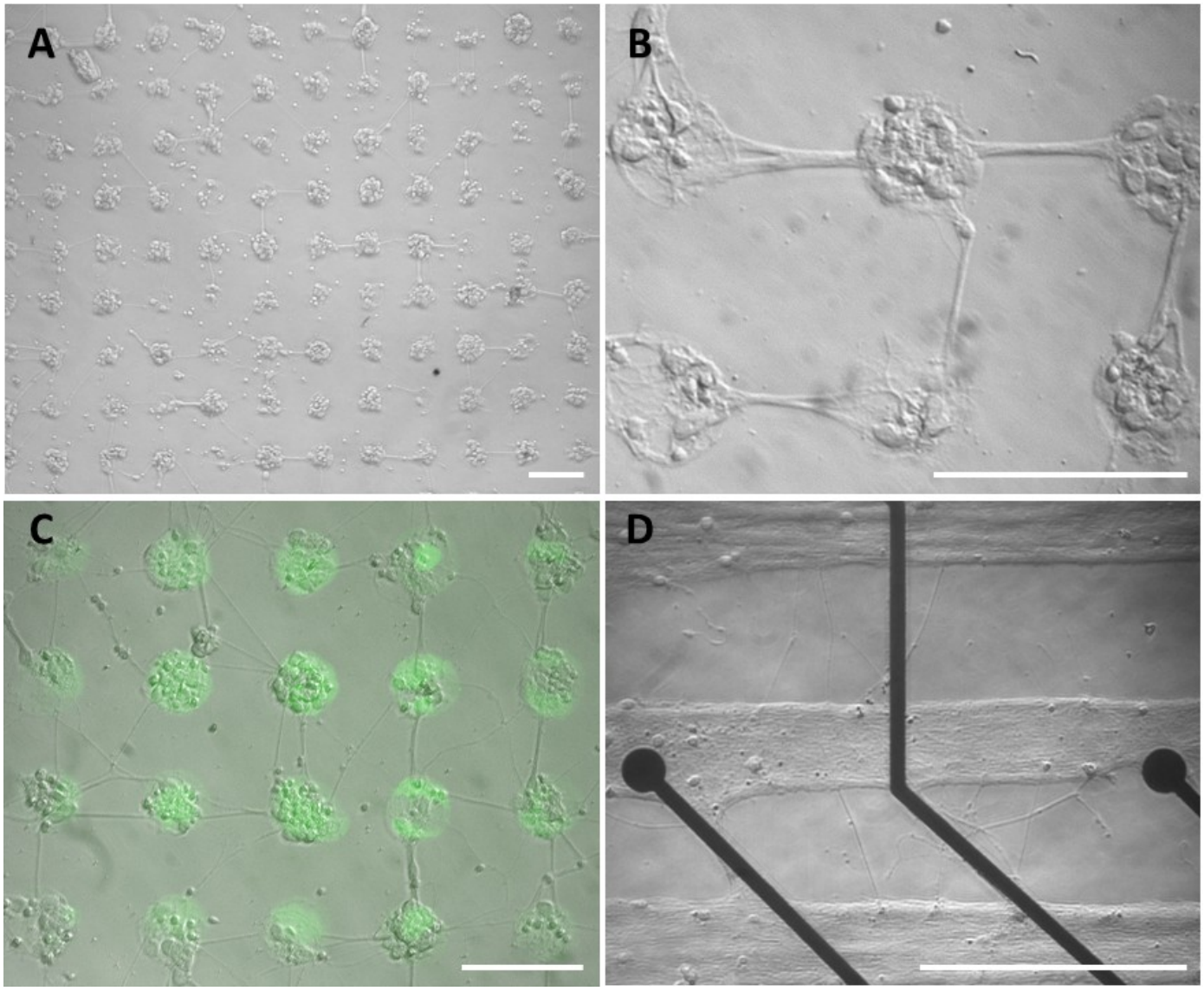

Fig. 1. Rat cortical neurons on printed poly-L-lysine patterns. (A,B) Light microscopy images of neurons at 5 DIV on P:DLC. (C) Merged light/fluorescence microscopy image showing neurons and FITC-tagged poly-L-lysine on P:DLC (green). (D) Rat cortical neurons grown on poly-L-lysine lines printed on to an MEA (6 days *in vitro*). Scale bars: 100 µm.

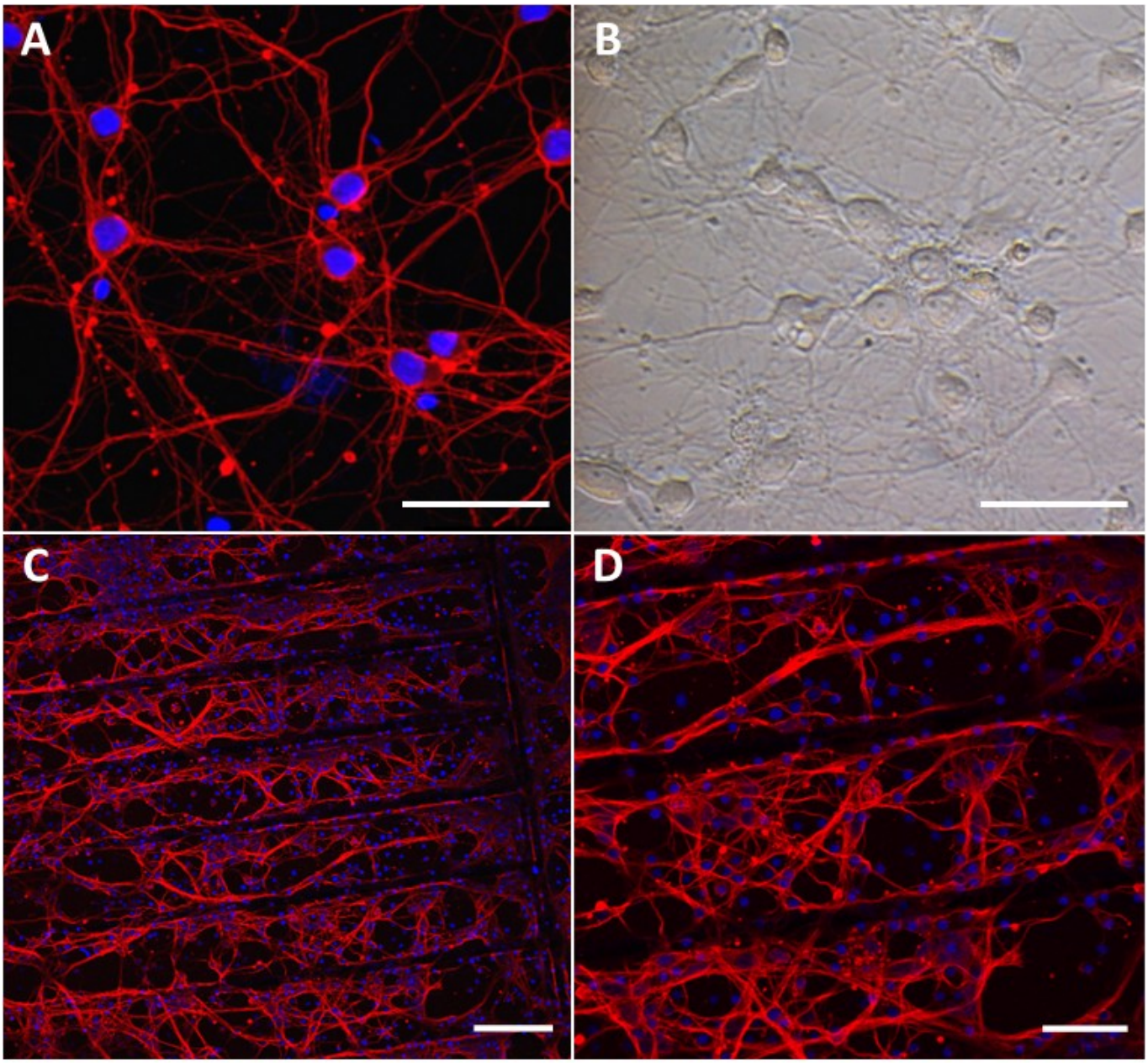

Fig. 2. Rat cortical neurons seeded on (A) boron-doped diamond and (B) TCPS. (C) Neurons on boron-doped diamond following laser micromachining (rectangular array). Cells were phenotyped utilising immunocytochemistry incorporating the neuronal marker, beta-III-tubulin (red), and the nuclear stain, DAPI (blue). All images were taken at 7 days *in vitro*. Scale bars: 50 μm (A, B and D), (C) 100 μm.

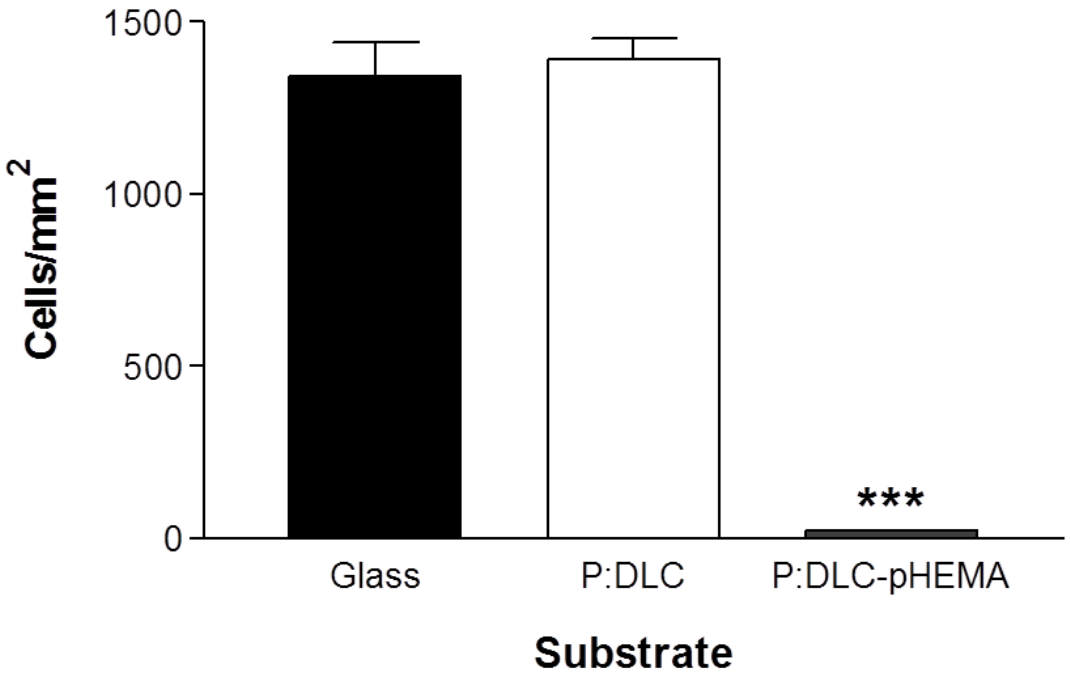

Fig. 3. Cell counts of adhered bone-marrow derived macrophages on glass, P:DLC and polyHEMA coated P:DLC (P:DLC-pHEMA) at 1 day *in vitro*. Error bars represent standard error of the mean values as determined from three independent experiments (n = 9). Asterisks indicate a significant difference from control (glass) by one-way analysis of variance ANOVA with Bonferroni's multiple comparison test (*** $p \leq 0.001$).

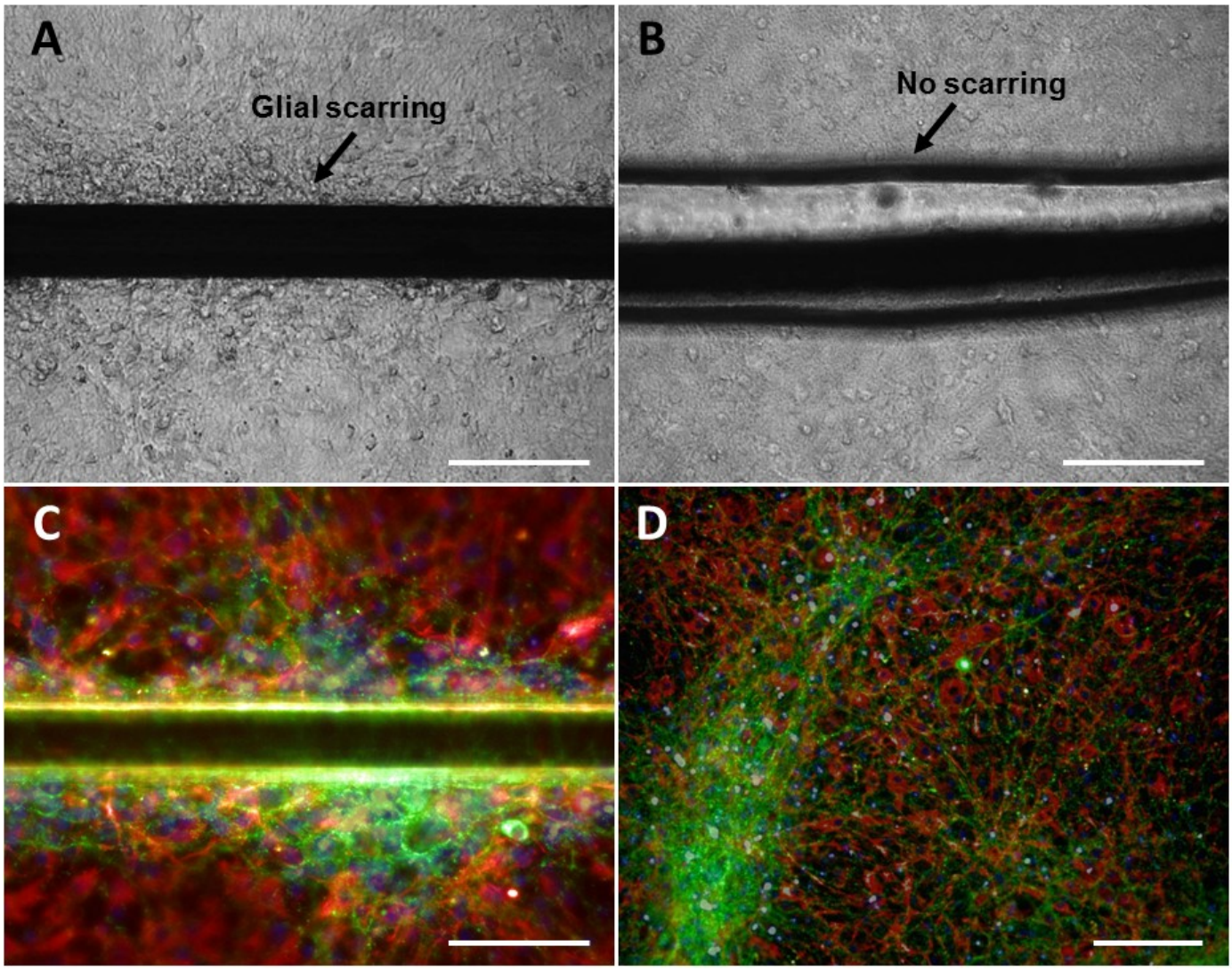

Fig. 4. Cell responses to microwires placed in a mixed culture of neurons, astrocytes and microglia. (A) P:DLC coated NiCr wire. (B) P:DLC-pHEMA-coated NiCr wire. Immunostained images are shown of the mixed cell culture containing (C) a P:DLC coated NiCr wire (focused onto the mid-way plane of the wire) and (D) the same culture conditions without a NiCr wire. Cells were phenotyped using immunocytochemistry incorporating the neuronal marker, beta-III-tubulin (red), the glial marker, GFAP (green) and the nuclear stain, DAPI (blue). Images are representative of data taken from $n = 9$ tests. Scale bars: 100 μm.

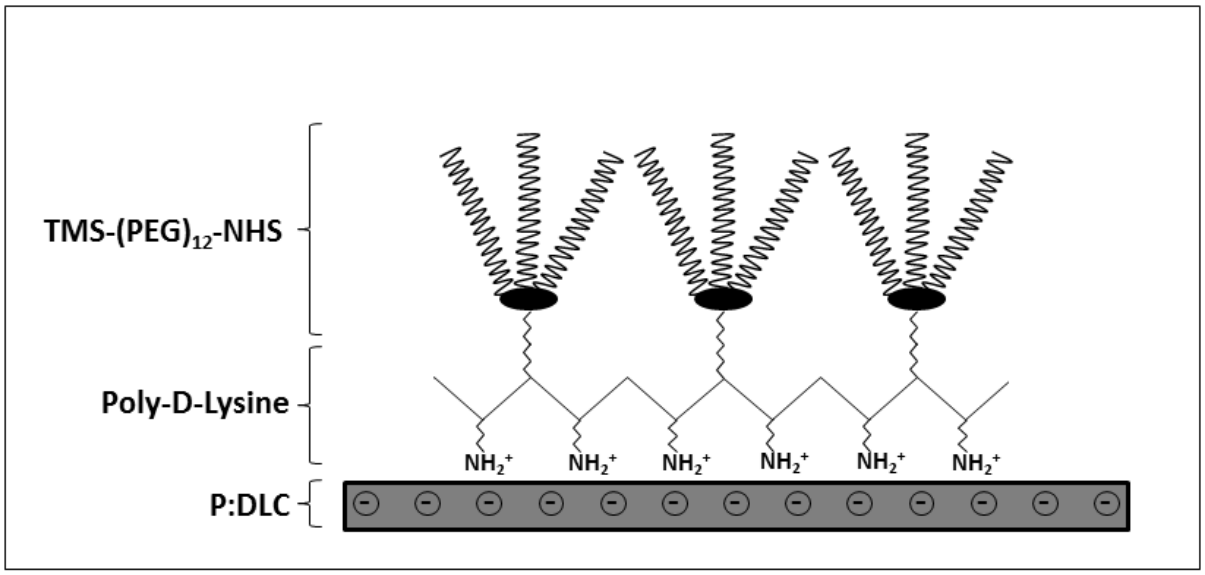

Fig. 5. The PEGylation method for P:DLC. Poly-D-lysine forms electrostatic bonds with the phosphate groups of P:DLC. The poly-D-lysine is then reacted with the amine-reactive TMS-$(PEG)_{12}$-NHS reagent to covalently attach surface PEG groups.

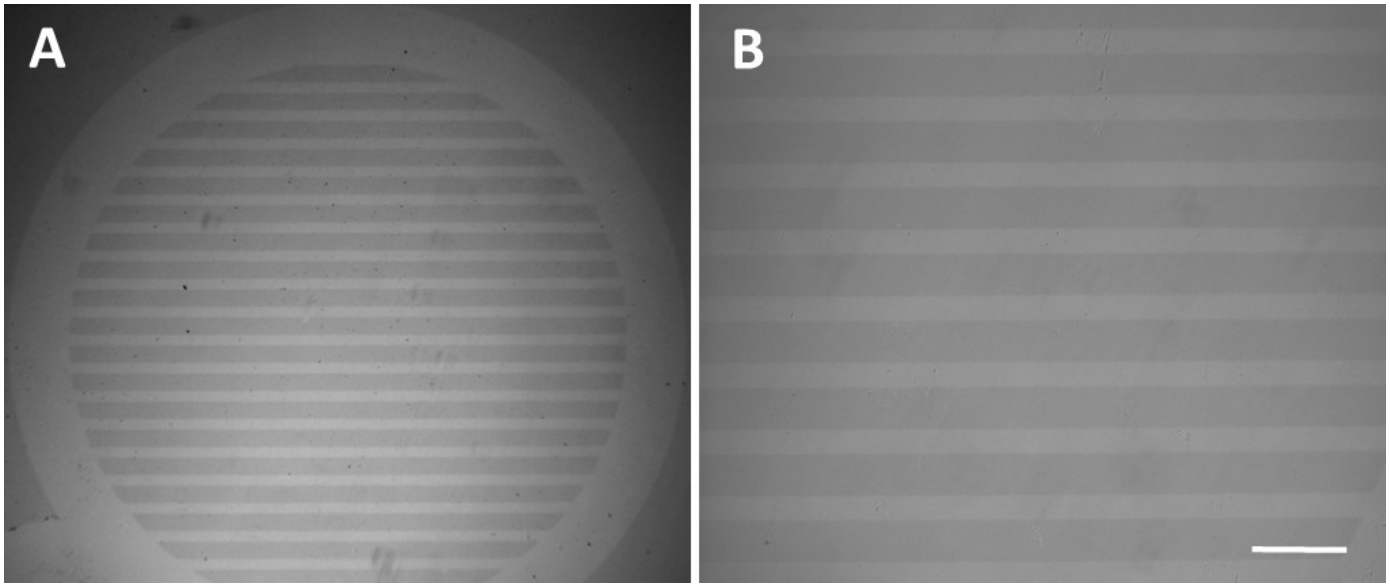

Fig. 6. Light microscopy images showing micropatterned P:DLC-DLC. (A) Parallel line pattern, low magnification. (B) Parallel line pattern, medium magnification. The outer circular diameter of each entire grid was 5 mm. Scale bar: 200 μm.

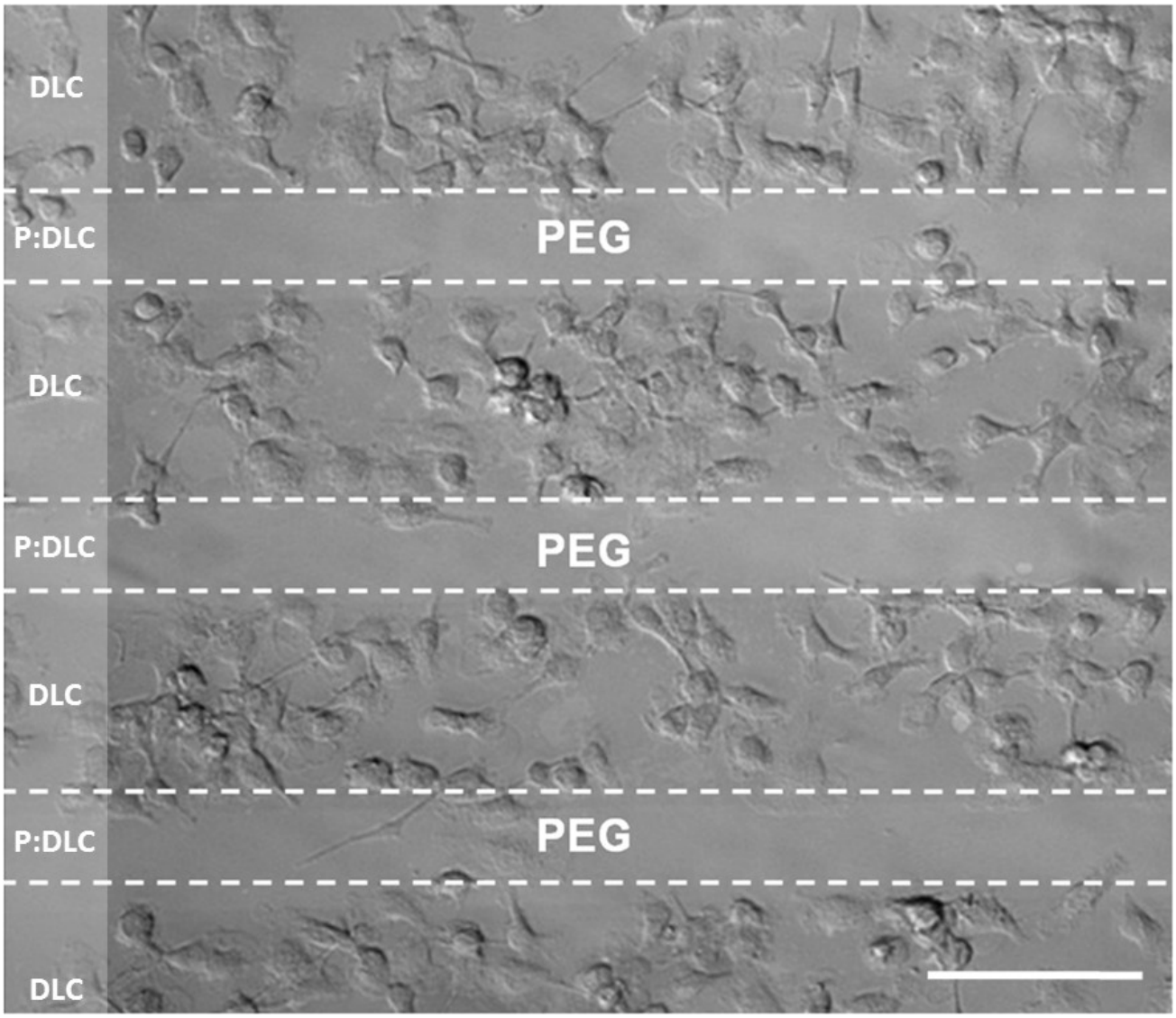

Fig. 7. Bone-marrow derived macrophages on PEGylated P:DLC-DLC patterned substrates. The areas containing PEG, P:DLC and DLC are highlighted (between white dashed lines). Scale bar: 90 μm.

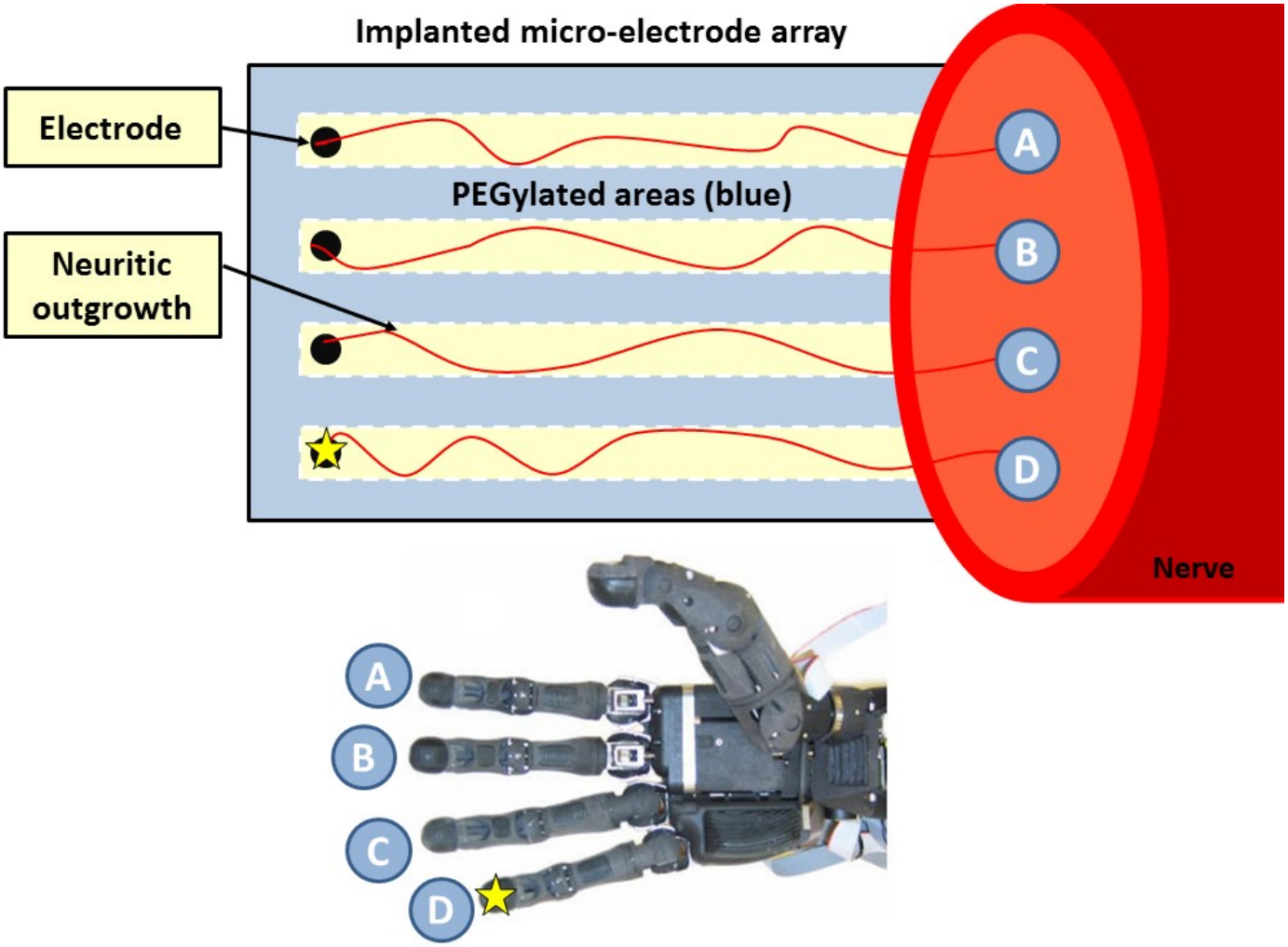

Fig. 8. The advantages of directing nerve and brain growth in neuro-prosthetics. Specific areas of the longitudinal nerve cross-section are thought to code for defined functions, *e.g.* individual digit movement. Therefore, maintaining the spatial organisation of the nerve (or brain) by directing neuritic outgrowth to specific electrodes, *e.g.* by patterned PEGylation, would reduce neural signal cross-talk. General coatings of PEG/pHEMA upon the implant would be expected to reduce the magnitude of the glial scar response and so aid improved neuron-electrode connectivity. A small degree of microglial and astrocytic growth on non-coated areas would, however, allow the positive benefits of these cells to influence neuronal health, such as removal of harmful cell debris and providing trophic support. By patterning neuronal growth, a reduction in electrical signal cross-talk would improve the level of neural control over a neuro-prosthetic interface, *e.g.* a nerve-signal controlled robotic hand. [53].